Eccentricity fluctuations are not the only source of elliptic flow fluctuations in a multiphase transport model *

Kai Xiao(肖凯)[1,2;1)] Feng Liu(刘峰)[1;2)] Fu-Qiang Wang(王福强)[1,3,4;3)]

[1]Key Laboratory of Quark and Lepton Physics (MOE) and Institute of Particle Physics, Central China Normal University, Wuhan 430079, China
[2]College of Electronics and Information Engineering, South-Central University for Nationalities, Wuhan 430074, China
[3]Department of Physics, Purdue University, West Lafayette, Indiana 47907, USA
[4]School of Science, Huzhou University, Zhejiang 313000, China

Abstract: Sources of event-by-event elliptic flow fluctuations in relativistic heavy-ion collisions are investigated in a multiphase parton transport model (AMPT). Besides the well-known initial eccentricity fluctuations, several other sources of elliptic flow dynamical fluctuations are identified. One is fluctuations in initial parton configurations at a given eccentricity. Configuration fluctuations are found to be as important as eccentricity fluctuations in elliptic flow development. A second is quantum fluctuations in parton-parton interactions during system evolution. A third is fluctuations caused by hadronization and final-state hadronic scatterings. The magnitudes of these fluctuations are investigated relative to the eccentricity fluctuations and the average elliptic flow magnitude. The fluctuations from the latter two sources are found to be negative. The results may have important implications for the interpretation of elliptic flow data.

Keywords: elliptic flow fluctuations, eccentricity, initial configuration, parton-parton interactions, hadronization and hadronic scatterings

PACS: 25.75.Gz, 21.65.Qr, 24.60.Ky **DOI:** 10.1088/1674-1137/41/9/094103

1 Introduction

A strongly interacting quark-gluon plasma (sQGP) is believed to be created in relativistic heavy-ion collisions [1]. At nonzero impact parameter, the transverse overlap region of colliding nuclei is anisotropic. Due to interactions among constituents, the produced matter undergoes a rapid anisotropic expansion resulting in an anisotropic distribution of final-state hadrons in momentum [2]. The elliptic anisotropy can be quantified by the second coefficient (v_2) of the Fourier expansion of the final-state particle azimuthal distribution, called elliptic flow [3]. Because the anisotropy in configuration space is quickly transferred into momentum space due to anisotropic expansion, elliptic flow is primarily sensitive to the early stage of sQGP evolution. Shear viscosity is known to damp the development of elliptic flow. Elliptic flow data, in comparison to hydrodynamical calculations, may therefore constrain the shear viscosity to entropy density ratio (η/s) [4].

Elliptic flow has been extensively studied experimentally [1] and theoretically [5]. Because the details of initial-state geometry are not experimentally accessible, elliptic flow is often measured by two-particle correlations [6]. The measured quantity is the mean square, $\langle v_2^2 \rangle$, where $\langle ... \rangle$ is the average over all the events. Event-by-event elliptic flow fluctuations are therefore critical and the understanding of these fluctuations is essential in extracting physics information from elliptic flow measurements utilizing correlation techniques.

At a given impact parameter (b), the interacting nucleons are not identically distributed event-by-event due to fluctuations in nucleon distribution in a nucleus and due to the quantum nature of nucleon-nucleon interactions. As a consequence, elliptic flow develops relative to the so-called participant plane [7, 8], not the reaction plane defined by the beam and impact parameter directions. It is believed that elliptic flow fluctuations

Received 20 January 2017, Revised 11 May 2017

∗ Supported by MOST, China, under 973 Grant 2015CB856901, National Natural Science Foundation of China (11521064, 11547143, 11228513), U.S. Department of Energy (DE-FG02-88ER40412), Fundamental Research Funds for the Central Universities, South-Central University for Nationalities (CZQ15001) and Excellent Doctorial Dissertation Cultivation Grant from Central China Normal University (2013YBZD18)

1) E-mail: kxiao@mails.ccnu.edu.cn

2) E-mail: fliu@mail.ccnu.edu.cn

3) E-mail: fqwang@purdue.edu

are determined by fluctuations in the initial-state geometry configurations [9]. The initial-state geometry configuration is often quantified by eccentricities. In many elliptic flow studies, the final-state anisotropy is assumed to be proportional to the eccentricity. This proportionality, under the assumption of Gaussian fluctuations in the x and y components of eccentricity, leads to a Bessel-Gaussian form in the final-state elliptic flow coefficient v_2 [8]. However, at a given eccentricity and impact parameter, there can still be fluctuating distributions of interacting nucleons [7, 9]. Are these fluctuations important for elliptic flow development? This article tries to answer this question.

Given a fixed initial condition of participant configurations (x, y), not simply eccentricities, the hydrodynamical evolution is determined. Subsequently, the final state anisotropy from hydrodynamical calculations is fixed. However, there may be still other sources of dynamical fluctuations during the stages of system evolution, e.g. parton-parton interactions and hadronic scatterings, which could lead to additional elliptic flow fluctuations. Several authors have studied the fluctuations in the initial conditions and the consequent fluctuations in the final-state harmonic flows [10, 11]. This article further attempts to address this question by employing A Multi-Phase Transport (AMPT) [12] model with string melting, because transport models inherit all quantum (stochastic) fluctuations in the interactions among constituents.

2 Analysis method

AMPT describes many experimental data reasonably well, particularly the elliptic flow measurements [13]. It consists of four main parts: the initial condition, parton-parton interactions, hadronization, and hadronic scatterings. The initial condition is obtained from the HIJING model [14], which includes the spatial and momentum information of minijet partons from hard processes and strings from soft processes. The time evolution of partons is then treated according to the ZPC parton cascade model [15]. After parton interactions cease, a combined coalescence and string fragmentation model is used for the hadronization of partons. The subsequent scatterings among the resulting hadrons are described by the ART model [16], which includes both elastic and inelastic scatterings.

The initial geometric anisotropy of the transverse overlap region of a heavy-ion collision is often described by the eccentricity [17]:

$$\varepsilon_n=\frac{\sqrt{\langle r^n\cos(n\phi_r)\rangle^2+\langle r^n\sin(n\phi_r)\rangle^2}}{\langle r^n\rangle}, \tag{1}$$

where r and ϕ_r are the polar coordinate positions of each parton liberated by the initial encounter of the colliding nuclei, n refers to the $n^{\rm th}$ harmonic, and $\langle ...\rangle$ is the average over all the partons in an event. Note that various radial weights (e.g. r^2 vs r^n) are used in the literature to quantify the initial geometry eccentricities [18, 19]. For the elliptic flow we focus on in this study, we use Eq. (1), which is the most common definition.

As the system evolves, the initial configuration anisotropy is transferred to momentum anisotropy by the hydrodynamical pressure gradient or strong interactions among constituents. The momentum anisotropy is widely characterized by the Fourier coefficients [6]:

$$v_n=\langle\cos[n(\phi-\Psi_n)]\rangle, \tag{2}$$

where ϕ is the particle azimuthal angle and Ψ_n is the $n^{\rm th}$ harmonic plane angle. In AMPT, Ψ_n can be calculated in coordinate space by [17]

$$\Psi_n^r=\frac{\text{atan2}(\langle r^n\sin(n\phi_r)\rangle,\langle r^n\cos(n\phi_r)\rangle)+\pi}{n}. \tag{3}$$

Here the superscript r in Ψ_n^r means Ψ_n^r is reconstructed by the initial parton distributions in coordinate space. We often call Ψ_n^r the participant plane. Note Ψ_n^r is not necessarily the reaction plane due to event-by-event geometry fluctuations. Due to the finite multiplicity of constituents, the estimated harmonic plane is smeared from the true one – the geometric harmonic plane of the participant partons in configuration space in the limit of infinite parton multiplicity – by a resolution factor. The resolution factor is calculated with an iterative procedure by the subevent method, dividing the constituents randomly into two subevents [6]. Because of the large initial parton multiplicity (averages 16220, 12520 and 5703 for b = 0 fm, 4 fm and 8 fm, respectively), the calculated resolution is nearly unity [20].

Experimentally, the configuration space harmonic plane is inaccessible. Used as a proxy is the event plane reconstructed from final-state particle momenta. However, the event plane is contaminated by nonflow (particle correlations unrelated to the symmetry harmonic plane). In order to study only the collective anisotropic flow, not contaminated by nonflow, we use the configuration space harmonic plane in AMPT to obtain the elliptic flow as our main result.

However, we also use the 2-particle and 4-particle cumulant methods, as same as in experimental data analysis, to calculate elliptic flow. Because of their different sensitivities to v_2 fluctuations, the 2- and 4-particle cumulants can be used to estimate v_2 fluctuations.

3 Results and discussion

Figure 1(a)–(c) shows the event-by-event correlations between v_2 of partons after parton interactions cease and before hadronization occurs, and ε_2 from the ini-

tial collision geometry at three fixed impact parameters. Figure 1(d)–(f) shows event-by-event correlations between v_2 of final-state charged hadrons after hadronic scatterings and the same ε_2. The relation between ε_2 and v_2 has been investigated by hydrodynamical calculations [10, 11, 18, 19, 21], which provides a foundation for the understanding of v_2 data. Studies of how event-by-event fluctuations in the initial stages manifest in the final state correlations have been reviewed in Ref. [22]. Before studying v_2 fluctuations, it is useful to first examine the behavior of average $\langle v_2\rangle$ vs. ε_2. This is shown in Fig. 1 by the solid dots. As ε_2 increases, the magnitude of average $\langle v_2\rangle$ increases linearly. The conversion coefficient (k), the slope of $\langle v_2\rangle$ vs. ε_2 from a linear fit to the data, appears compatible between $b = 0$ and 4 fm and smaller for $b = 8$ fm. Interestingly, at a given b, almost the same k is observed for parton and hadron v_2 vs. ε_2. This indicates that the final-stage hadronic scatterings in AMPT do not generate significant additional v_2.

Large fluctuations in ε_2 are observed in Fig. 1, which are due to geometry fluctuations at a fixed b. The fluctuations in ε_2 are given by $\sigma_{\varepsilon_2} = \sqrt{\langle\varepsilon_2^2\rangle - \langle\varepsilon_2\rangle^2}$ and $\langle ...\rangle$ indicates an average over all events. Because of the large number of initial partons used to determine ε_2, the statistical fluctuation effect on ε_2 is negligible. For central collisions ($b = 0$ fm), the magnitude of relative eccentricity fluctuations ($\sigma_{\varepsilon_2}/\langle\varepsilon_2\rangle$) is found to be 0.52, in agreement with the finding in Ref. [23]. With increased b, the ε_2 fluctuations are larger. For a given ε_2, however, there still exist wide dispersions in v_2. This indicates that v_2 fluctuations are not solely due to ε_2 fluctuations; there are additional fluctuation sources in v_2. One source is simply statistical fluctuations (and they are larger in hadron v_2 than parton v_2 mainly due to the smaller number of hadrons than partons). We define the statistical fluctuations of v_2 as $\sigma_{v_2}\{\text{sta}\}$. Any fluctuation beyond the statistical fluctuation is called dynamical fluctuation:

$$W_{\text{dyn}} = \sigma_{v_2}^2 - \sigma_{v_2}^2\{\text{sta}\}, \tag{4}$$

where σ_{v_2} is the total fluctuation. There may be sources of dynamical fluctuations in v_2.

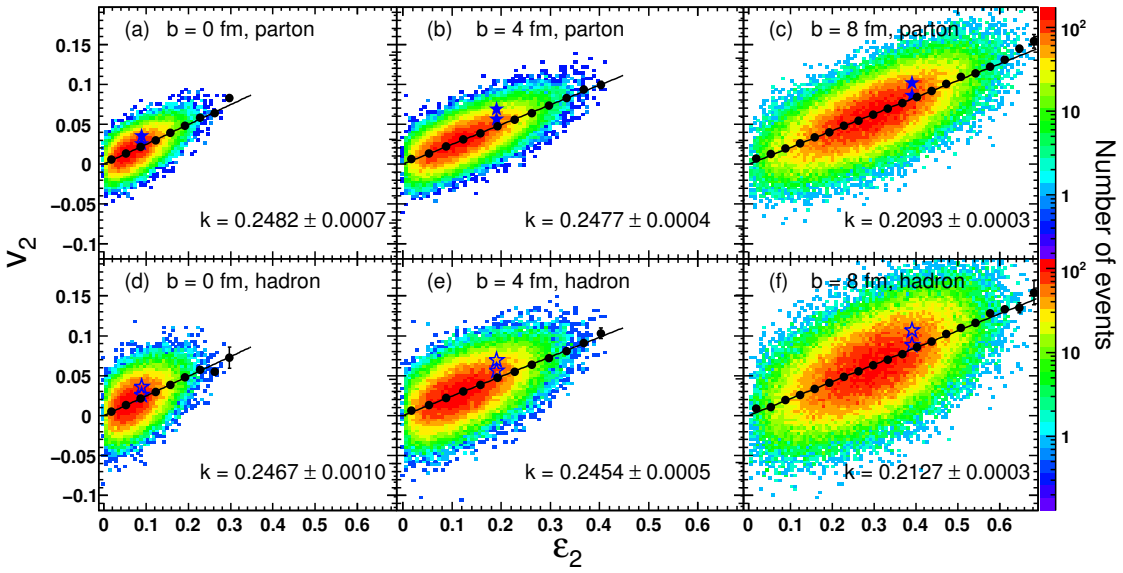

Fig. 1. (color online) Event-by-event correlations between elliptic flow v_2 and initial configuration eccentricity ε_2 for three different impact parameters (b=0 fm, 4 fm and 8 fm) in Au+Au collisions at $\sqrt{s_{\text{NN}}}$ = 200 GeV using the AMPT model (3 mb parton-parton cross section). (a-c) and (d-f) show v_2 of partons and charged hadrons, respectively, both within a pseudo-rapidity of $|\eta| < 1.0$ and $p_{\text{T}} < 2.0$ GeV/c. The solid dots show the behavior of average $\langle v_2\rangle$ vs. ε_2 and the lines are one-parameter fits to $v_2 = k\times\varepsilon_2$. See the main text for the explanation of the twelve stars in the panels.

We first investigate fluctuations in initial parton configurations at fixed eccentricity. The same ε_2 does not necessarily mean the same initial configuration of partons – two events of different initial configurations can give identical ε_2. This may cause fluctuations in v_2, if v_2 is sensitive to the initial configuration, not simply ε_2. We define this part of fluctuations as $W_{\text{dyn}}\{\text{cfg}\}$. The stars in Fig. 1 show the averaged v_2 with identical ε_2 (we take the eccentricities to be the same if they fall into the same bin, with bin size 0.001) from two different sets of events. Each set consists of 3000 events, starting from an identical configuration of initial partons. That is, AMPT

starts with exactly identical parton configuration (events have the same initialization), and then evolves with different random number seeds. The different average $\langle v_2\rangle$s demonstrate that the fluctuations observed in Fig. 1 are not due to statistical fluctuations only; fluctuations in the initial conditions are important.

The spread of v_2 in Fig. 1 at a given ε_2 is made up from spreads of event-by-event v_2's of the different initial configurations about the corresponding average $\langle v_2\rangle$'s. The spread of v_2 for a fixed initial condition (identical parton configurations) comes from statistical fluctuations and possibly other dynamical fluctuations. One source of such dynamical fluctuations can be quantum fluctuations in parton-parton interactions. We define this part of the fluctuations as $W_{\rm dyn}\{\rm par\}$. In the case of hadron v_2, additional fluctuations can arise from hadronization and final-state hadronic scattering processes. We define this part of the fluctuations as $W_{\rm dyn}\{\rm had\}$.

We now study quantitatively v_2 fluctuations from the various sources. AMPT is run with default settings and with fixed initial conditions. The v_2 fluctuations of partons and hadrons, at a given eccentricity, are obtained from these two ways of running. The fluctuations from the default setting run are $\sigma_{v_2}\{\rm par{+}cfg{+}sta_{parton}\}$ and $\sigma_{v_2}\{\rm had{+}par{+}cfg{+}sta_{hadron}\}$ for partons and hadrons, respectively, and those from the fixed initial conditions run are $\sigma_{v_2}\{\rm par{+}sta_{parton}\}$ and $\sigma_{v_2}\{\rm had{+}par{+}sta_{hadron}\}$. The fluctuations are calculated by

$$\sigma_{v_2}=\sqrt{\langle v_2^2\rangle-\langle v_2\rangle^2}, \tag{5}$$

where v_2 is the magnitude of elliptic flow in a single event, given by Eq. (2) and $\langle ...\rangle$ indicates an average over all events at a chosen ε_2.

Figure 2(a)–(c) shows the v_2 fluctuations as a function of ε_2. In order to obtain the dynamical fluctuations, the statistical fluctuations due to finite multiplicities need to be subtracted. The statistical smearing may be determined by an unfolding procedure [24]. In our study, the statistical fluctuations of v_2 are calculated by

$$\sigma_{v_2}\{\rm sta\}=\sqrt{\frac{\langle\cos^2(2\phi)\rangle-\langle\cos(2\phi)\rangle^2}{N}}=\sqrt{\frac{1-2\langle v_2\rangle^2}{2N}}. \tag{6}$$

This is verified by a Monte Carlo toy model where N particles are generated with ϕ angles between 0 and 2π according to a v_2 modulation [23, 25]. We also use the AMPT data themselves to obtain the statistical fluctuation effect by randomly discarding various fractions of particles. The v_2 fluctuations of the remaining fraction (f) of particles are fit to the functional form of $\sqrt{W_{\rm dyn}+\sigma^2_{v_2}\{\rm sta\}/f}$, where $W_{\rm dyn}$ and $\sigma_{v_2}\{\rm sta\}$ are two free parameters. The fitted $\sigma_{v_2}\{\rm sta\}$ is found to be consistent with Eq. (6).

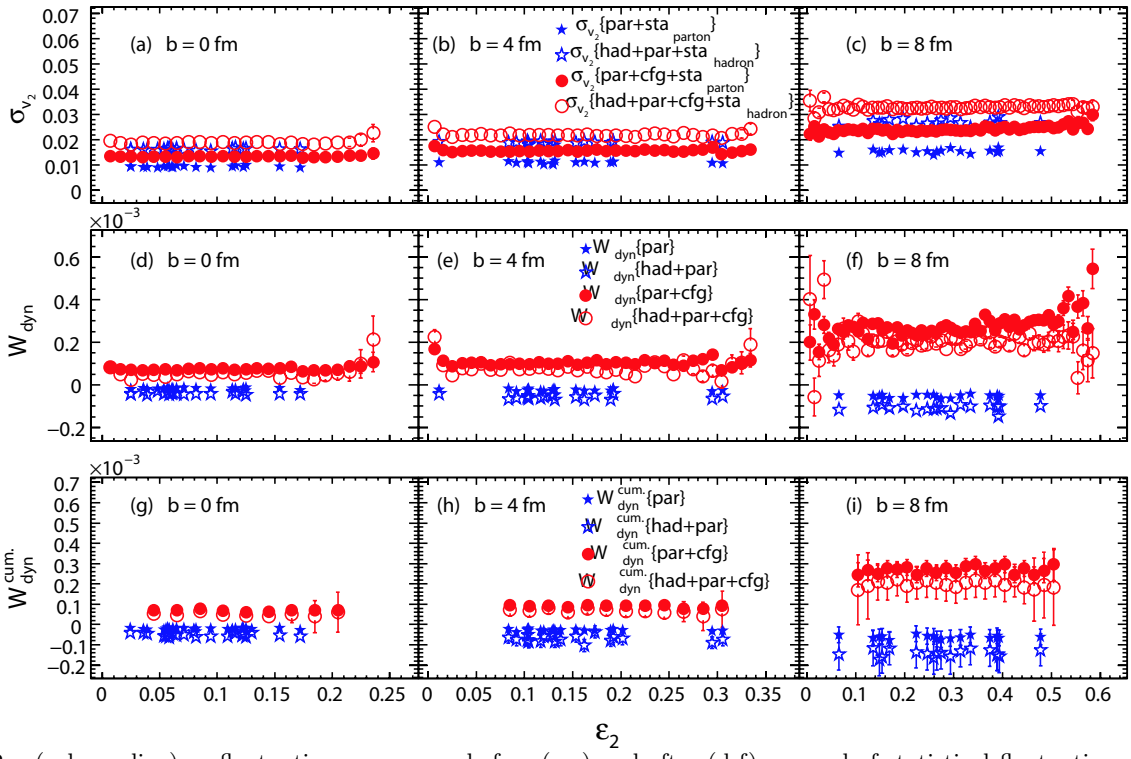

Fig. 2. (color online) v_2 fluctuations versus ε_2, before (a-c) and after (d-f) removal of statistical fluctuations. Red points are from the default settings (from Fig. 1), while the blue points are from runs with identical parton configuration (examples shown in stars in Fig. 1) in Au+Au collisions at $\sqrt{s_{\rm NN}}=200$ GeV by the AMPT model. (g-i) show the corresponding v_2 fluctuations obtained by the 2- and 4-particle cumulant methods.

We subtract the statistical fluctuations given by Eq. (6) from the data in Fig. 2(a)–(c). The resulting dynamical fluctuations are shown in Fig. 2(d)–(f). It is found that the dynamical fluctuations for the fixed initial condition data, corresponding to the $W_{\rm dyn}\{\rm par\}$ and $W_{\rm dyn}\{\rm had+par\}$ in Eq. (4) and in the fit function mentioned above, are both negative. The latter is larger than the former in terms of magnitude. This suggests that parton-parton interactions and hadronization+hadronic scatterings both introduce negative dynamical fluctuations.

In order to gain more insights, we obtain the v_2 fluctuations, alternatively, from the 2- and 4-particle cumulant methods. As mentioned in Section 2, the 2- and 4-particle cumulants have different sensitivities to v_2 fluctuations and can therefore yield information on v_2 fluctuations. One complication is that the 2-particle cumulant is contaminated by nonflow although nonflow is strongly suppressed in the 4-particle cumulant. However, when nonflow effects are negligible for the 2-particle cumulant, which is generally the case at low $p_{\rm T}$ in AMPT, and if v_2 fluctuations are relatively small compared to the average v_2 value, $\sigma_{v_2} \ll \langle v_2\rangle$, the 2-particle and 4-particle cumulants up to the order $\sigma^2_{v_2}$ are given by

$$v_2\{2\}^2 = \langle v_2\rangle^2 + W^{\rm cum.}_{\rm dyn}, \tag{7}$$

$$v_2\{4\}^2 = \langle v_2\rangle^2 - W^{\rm cum.}_{\rm dyn}, \tag{8}$$

where $W^{\rm cum.}_{\rm dyn}$ is the dynamical v_2 fluctuations. The dynamical v_2 fluctuations can be obtained from the cumulant method as

$$W^{\rm cum.}_{\rm dyn} = \sigma^2_{v_2,{\rm dyn}} = (v_2\{2\}^2 - v_2\{4\}^2)/2 \tag{9}$$

The fluctuations from the default setting run are $W^{\rm cum.}_{\rm dyn}\{\rm par+cfg\}$ and $W^{\rm cum.}_{\rm dyn}\{\rm had+par+cfg\}$ for partons and hadrons, respectively, and those from the fixed initial-condition run are $W^{\rm cum.}_{\rm dyn}\{\rm par\}$ and $W^{\rm cum.}_{\rm dyn}\{\rm had+par\}$. They are shown in Fig. 2(g-i). The v_2 fluctuations from the cumulant method in Fig. 2(g-i) are consistent with those obtained previously in Fig. 2(d-f). $W^{\rm cum.}_{\rm dyn}\{\rm par\}$ and $W^{\rm cum.}_{\rm dyn}\{\rm had+par\}$ from the cumulant method are also negative.

The negative dynamical v_2 fluctuations due to parton-parton interactions, hadronization and hadronic rescatterings in AMPT are one of the interesting results from our study. It is unexpected and the underlying physics is intriguing. We refer the reader to the Appendix, where we make the analogy of particle fusion to discuss what underlying physics might be responsible for the negative v_2 dynamical fluctuations from hadronization and hadronic inelastic scatterings. For the negative fluctuations from parton-parton elastic scatterings in AMPT, we speculate that under the extreme of an infinite number of scatterings, all particles should oriented in the short-axis direction and v_2 should be unity with zero spread. This would give negative fluctuations. The negative v_2 dynamical fluctuations may also exist in viscous hydrodynamic calculations, as shear viscosity could reduce flow and flow fluctuations [26, 27]. We note that all the v_2's are calculated relative to the same participant plane in configuration space at the initial time (defined by Eq. (3)). This follows the common practice in the studies of initial geometry and subsequent flow development [17], bearing in mind that initial geometry is the driving force for flow. It is, however, possible that the spatial distributions of constituents changes with time, and that v_2 could be defined with the instantaneous participant plane. This could result in different v_2 fluctuations. In addition, η/s reduces both $\langle v_2\rangle$ and σ_{v_2}, and if the reductions are different, one could obtain negative fluctuations.

As seen in Fig. 2, the fluctuations, while impact parameter dependent, are approximately independent of ε_2 at a given b. This is true for results both with and without statistical fluctuations subtracted (the multiplicities are found to be insensitive to the event-by-event ε_2 at a given b), as well as the cumulant results. We fit the results in Fig. 2(d-i) to a constant at each b. From the fitted values, we obtain the individual components of v_2 fluctuations by assuming the different sources of fluctuations are independent of each other, namely

$$W_{\rm dyn}\{A+B\} = W_{\rm dyn}\{A\} + W_{\rm dyn}\{B\}, \tag{10}$$

where A and B stand for two independent fluctuation sources. There are redundancies in the data in Fig. 2. For example, one can obtain $W_{\rm dyn}\{\rm cfg\}$ by taking the difference either between $W_{\rm dyn}\{\rm par+cfg\}$ and $W_{\rm dyn}\{\rm par\}$ or between $W_{\rm dyn}\{\rm had+par+cfg\}$ and $W_{\rm dyn}\{\rm had+par\}$; similarly for the $W^{\rm cum.}_{\rm dyn}$ fluctuations. They all give consistent results. Conversely, this indicates that our independent source assumption in Eq. (10) is reasonable.

Figure 3(a) shows v_2 fluctuations due to initial configuration fluctuations as a function of b. $W_{\rm dyn}\{\rm cfg\}$ and $W^{\rm cum.}_{\rm dyn}\{\rm cfg\}$ are quantitatively consistent with each other. The contributions from eccentricity fluctuations, $W_{\rm dyn}\{\varepsilon_2\} = \sigma^2_{v_2}\{\varepsilon_2\} = k^2\times\sigma^2_{\varepsilon_2}$, are also shown, where the conversion power (multiplicative factor k) from ε_2 to v_2 is obtained from the fits in Fig. 1. $W_{\rm dyn}\{\rm cfg\}$ and $W_{\rm dyn}\{\varepsilon_2\}$ are comparable in magnitude. They are found to increase with increasing b. The increase is nearly equally strong. The results suggest that configuration fluctuations are as important as eccentricity fluctuations. Figure 3(b) shows v_2 fluctuations due to parton-parton interactions and hadronization and final-state hadronic scatterings as a function of b. Again, $W_{\rm dyn}\{\rm par\}$ and $W_{\rm dyn}\{\rm had\}$ are quantitatively consistent with the corresponding cumulant results, $W^{\rm cum.}_{\rm dyn}\{\rm par\}$ and $W^{\rm cum.}_{\rm dyn}\{\rm had\}$, respectively. They are both negative and have weak dependence on b. Our results indicate that parton-parton interactions and

hadronization and final-state hadronic scatterings cause negative dynamical v_2 fluctuations.

Figure 4(a) shows the ratio of total v_2 fluctuations to $\sigma_{v_2}\{\varepsilon_2\}$, the contribution from eccentricity fluctuations. Clearly, the total v_2 fluctuations in AMPT are larger than eccentricity fluctuations, and there does not seem to be a simple scaling between eccentricity fluctuations and total v_2 fluctuations. Figure 4(b) shows the negative dynamic fluctuations relative to $\langle v_2\rangle^2$ as a function of b. The relative magnitudes decrease (smaller absolute value) with increasing b, which is qualitatively consistent with weaker interactions at larger b that yield smaller negative relative fluctuations.

v_2 is mainly proportional to ε_2, though nonlinearity is not zero [10]. It is often considered that v_2 fluctuations are dominated by ε_2 fluctuations [11]. Our study shows, within the framework of AMPT, that this may not be the case. Those other v_2 fluctuations can be important and they do not seem to scale with eccentricity fluctuations. We note that these additional elliptic flow fluctuations are not unique to AMPT, but should also present in other transport models, such as UrQMD [28].

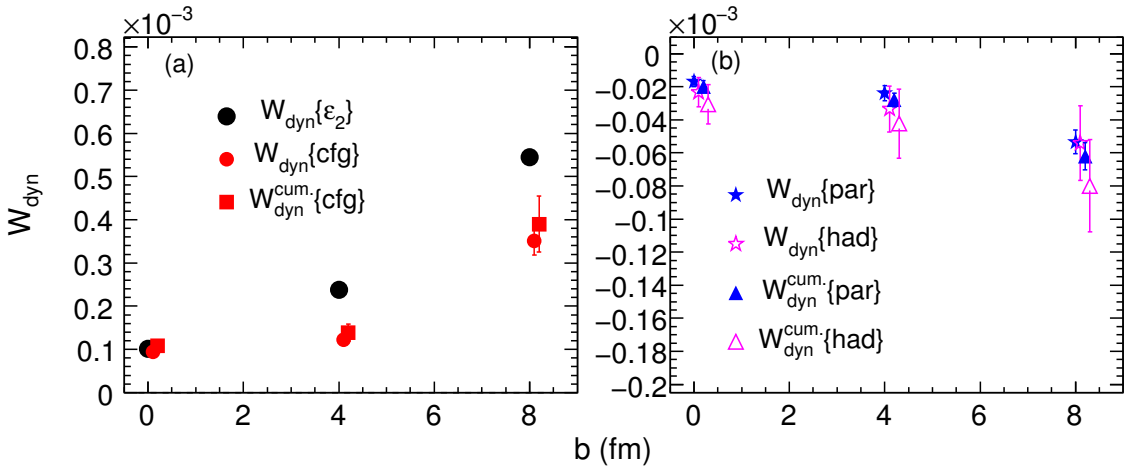

Fig. 3. (color online) Impact parameter dependence of v_2 fluctuations due to (a) eccentricity fluctuations and initial configuration fluctuations and (b) parton-parton interactions and hadronization and final-state hadronic scatterings in Au+Au collisions at $\sqrt{s_{\rm NN}}$ = 200 GeV using the AMPT model. The fluctuations obtained from the cumulant method are also shown. Three b values (0, 4, 8 fm) are studied but the data points are shifted in b for clarity.

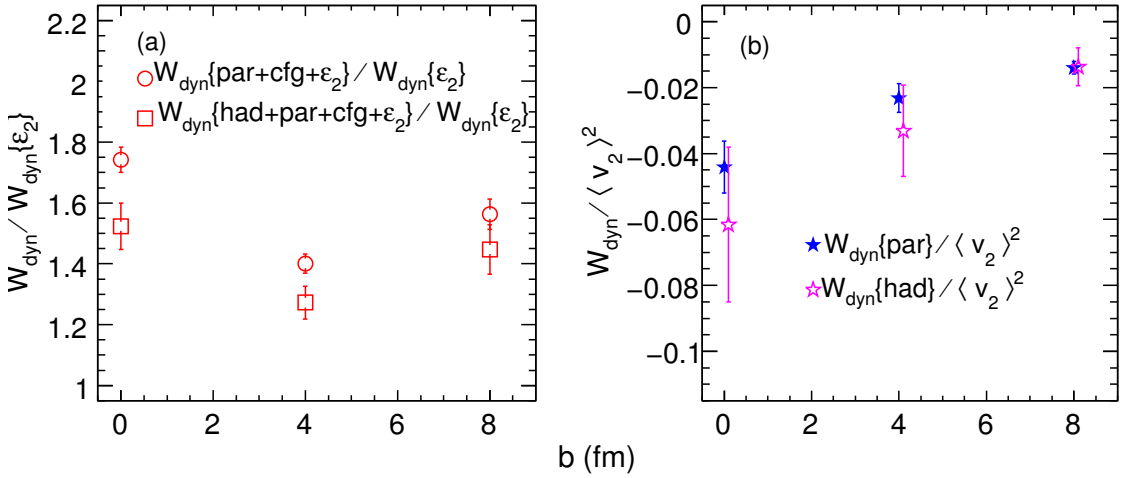

Fig. 4. (color online) Impact parameter dependence of (a) ratio of total v_2 fluctuations to eccentricity fluctuations and (b) various v_2 fluctuations relative to averaged $\langle v_2\rangle^2$ in Au+Au collisions at $\sqrt{s_{\rm NN}}$ = 200 GeV using the AMPT model. Three b values (0, 4, 8 fm) are studied but the data points are shifted in b for clarity.

Hydrodynamical calculations of v_2 do not have any other fluctuations except initial geometry fluctuations (the sum of eccentricity fluctuations and initial configuration fluctuations). If our conclusion is correct that parton interactions, hadronization and final-state hadronic interactions introduce a negative dynamical v_2 fluctuation effect, and such an effect is relevant in real collision data, then hydrodynamics should have overpredicted v_2 data. Recently, fluctuations in hydrodynamics, governed by the viscosities, have been investigated [26, 27] and have been shown to be important and affect the elliptic flow fluctuations besides the initial state fluctuations. This source of fluctuations may be similar in nature to that in parton-parton interactions studied in this work.

4 Conclusions

Elliptic flow and fluctuations have been studied using the AMPT model with string melting at three fixed impact parameters in Au+Au collisions at $\sqrt{s_{\rm NN}} = 200$ GeV. Both v_2 of partons and hadrons with respect to the initial participant plane were studied. The average v_2 is linearly correlated with the average ε_2. There is a wide dispersion in v_2 for a given ε_2; v_2 is not solely determined by ε_2. Several dynamical fluctuation sources have been identified: initial configuration fluctuations at fixed ε_2, quantum fluctuations in parton-parton interactions, and fluctuations in hadronization and hadronic scatterings. The fluctuations were studied quantitatively by comparing the v_2 fluctuations from AMPT with default settings and with identical parton configuration, after subtraction of statistical fluctuations, as well as using the 2- and 4-particle cumulant method. The v_2 fluctuations due to configuration fluctuations are as large as those due to ε_2 fluctuations. They appear independent of ε_2 for a given b, and increase with increasing b. The dynamical fluctuations in v_2 from parton-parton interactions and hadronization and hadronic scatterings are found to be negative; they reduce overall v_2 fluctuations. The total v_2 fluctuations are larger than the eccentricity fluctuations and they do not seem to scale.

Hydrodynamical models have been very successful in describing experimental data. Most hydrodynamic calculations are deterministic; given an initial configuration space distribution, the final-state momentum anisotropy is fixed. Experimental data seem to be well described by eccentricity scaling and hydrodynamics. However, our study suggests that the configuration fluctuations do not seem to scale with eccentricity fluctuations, which suggests that the total v_2 fluctuations should not be strictly proportional to eccentricity fluctuations. Moreover, there can be additional sources of fluctuations, such as probabilistic parton-parton interactions, hadronization and hadronic rescatterings, that hydrodynamics do not take into account. Those other fluctuations potentially break the eccentricity scaling further. Our finding warrants further investigation of the physics mechanisms of elliptic flow fluctuations.

The authors thank You Zhou for useful suggestions.

Appendix A

Discussion on the negative dynamical fluctuations

In order to gain insights into the negative dynamical fluctuations, it is worth reminding ourselves that dynamical fluctuations are caused by correlations. An intuitive example is multiplicity fluctuation of a π gas from ρ^0 resonance decays. Suppose a system of N pairs of π^+ and π^- from N ρ^0 decays. The fluctuations of $2N$ π is $2\sqrt{N}$ because the fluctuations are due to the random fluctuations of N ρ^0. However, the final number of particles is $2N$ and the statistical fluctuations of $2N$ particles, assuming they are uncorrelated, is $\sqrt{2N}$. The dynamical fluctuation, $\sqrt{4N-2N} = \sqrt{2N}$, is therefore nonzero and positive. From the positive dynamical fluctuation we conclude that the particles are correlated, and the number of independent constituents (in this case, the ρ^0) is smaller. That is, multi-particle production from a single parent tends to introduce additional, i.e. positive, fluctuations (the particles are positively correlated). Taking this example in the opposite way, we may understand how negative fluctuations arise. Suppose a system of N particles are actually fused from $2N$ particles. The total fluctuation on N is $\sqrt{2N}/2$. The statistical fluctuation of the N particles, if all uncorrelated, is $\sqrt{N}$. The dynamical fluctuation $W_{\rm dyn}$ is $N/2-N = -N/2$, and negative.

The negative dynamical fluctuations in v_2 is less obvious than the simple multiplicity example. We used a toy model of particle fusing to test negative v_2 fluctuations. We generate $2N$ partons with an average v_2 by the AMPT model and group two adjacent partons (in ϕ) into one parton by adding their p_x's and p_y's together to become the p_x and p_y of the new parton. We then obtain the v_2 of the final N combined partons. We find the mean value and fluctuations of v_2 are as same as before; this is expected because the initial two particles of the same ϕ are now counted as just a single particle at that ϕ. However, the number of particles has now changed,

reduced by a factor of 2. The apparent statistical fluctuation is now larger than before and the dynamical fluctuation is negative. This is because now there are additional built-in correlations in the event: the v_2 fluctuation is really governed by the original number of particles, but we only measure the reduced number of particles in the final state. The negative dynamical fluctuations observed in AMPT due to hadronization and hadronic (inelastic) scatterings could be caused by fusing processes. Those processes tend to fuse particles into fewer ones. Indeed, hadronization in AMPT is modelled by parton coalescence, where two or three partons are coalesced into a hadron.

References

1 I. Arsene et al (BRAHMS Collaboration), Nucl. Phys. A, **757**: 1–27 (2005); B. B. Back et al (PHOBOS Collaboration), Nucl. Phys. A, **757**: 28–101 (2005); J. Adams et al (STAR Collaboration), Nucl. Phys. A, **757**: 102–183 (2005); S. S. Adcox et al (PHENIX Collaboration), Nucl. Phys. A, **757**: 184–283 (2005)
2 J. Y. Ollitrault, Phys. Rev. D, **46**: 229 (1992)
3 S. Voloshin and Y. Zhang, Z. Phys. C, **70**: 665 (1996)
4 P. Romatschke and U. Romatschke, Phys. Rev. Lett., **99**: 172301 (2007); U. Heinz, C. Shen, and H. C. Song, AIP Conf. Proc., **1441**: 766 (2012)
5 W. T. Deng, Z. Xu, and C. Greiner, Phys. Lett. B, **711**: 301–306 (2012); A. Bzdak and G. L Ma, Phys. Rev. Lett., **113**: 252301 (2014)
6 S. Wang et al, Phys. Rev. C, **44**: 1091 (1991); A. M. Poskanzer and S. A. Voloshin, Phys. Rev. C, **58**: 1671 (1998)
7 B. Alver et al (PHOBOS Collaboration), Phys. Rev. Lett., **98**: 242302 (2007)
8 S. A. Voloshin et al, Phys. Lett. B, **659**: 537–541 (2008)
9 S. Manly et al, Chinese Physics C, **31**: 1133–1136 (2007); B. Alver et al (PHOBOS Collaboration), Phys. Rev. C, **81**: 034915 (2010); B. Alver et al (PHOBOS Collaboration), Phys. Rev. Lett., **104**: 142301 (2010)
10 Z. Qiu, U. Heinz, Phys. Rev. C, **84**: 024911 (2011)
11 H. Niemi, G. S. Denicol, H. Holopainen, and P. Huovinen, Phys. Rev. C, **87**: 054901 (2013)
12 B. Zhang, C. M. Ko, B. A. Li, and Z. W. Lin, Phys. Rev. C, **61**: 067901 (2000)
13 Z. W. Lin, C. M. Ko, B. A. Li, B. Zhang, S. Pal, Phys. Rev. C, **72**: 064901 (2005)
14 X. N. Wang and M. Gyulassy, Phys. Rev. D, **44**: 3501 (1991)
15 B. Zhang, Comput. Phys. Commun., **109**: 193 (1998)
16 B. A. Li and C. M. Ko, Phys. Rev. C, **52**: 2037 (1995)
17 B. Alver and G. Roland, Phys. Rev. C, **81**: 054905 (2010)
18 D. Teaney and L. Yan, Phys. Rev. C, **83**: 064904 (2011)
19 F. G. Gardim et al, Phys. Rev. C **85**: 024908 (2012)
20 K. Xiao, F. Liu, and F. Wang, Phys. Rev. C, **87**: 011901(R) (2013)
21 G. Y. Qin, H. Petersen, S. A. Bass, and B. Muller, Phys. Rev. C, **82**: 064903 (2010); H. Petersen and B. Muller, Phys. Rev. C, **88**: 044918 (2013); W. L. Qian et al, J. Phys. G, **41**: 015103 (2014)
22 M. Luzum and H. Petersen, J. Phys. G, **41**: 063102 (2014)
23 W. Broniowski, P. Bozek, and M. Rybczynski, Phys. Rev. C, **76**: 054905 (2007)
24 A. R. Timmins et al (ALICE collaboration), J. Phys. Conf. Ser., **446**: 012031 (2013); G. Aad et al (ATLAS collaboration), Journal of High Energy Physics, **11**: 183 (2013)
25 S. Mrowczynski and E. Shuryak, Acta. Phys. Polon. B, **34**: 4241-4256 (2003)
26 C. Gale et al, Phys. Rev. Lett. **110**: 012302 (2013)
27 J. I. Kapusta, B. Muller, and M. Stephanov, Phys. Rev. C, **85**: 054906 (2012)
28 S. Vogel, G. Torrieri, and M. Bleicher, Phys. Rev. C, **82**: 024908 (2010)